Kinetics and Mechanism of the OH and OD Reactions with BrO

Yuri Bedjanian,* Véronique Riffault, Georges Le Bras, and Gilles Poulet†

Laboratoire de Combustion et Systèmes Réactifs, CNRS and Université d'Orléans, 45071 Orléans Cedex 2, France

Received: January 29, 2001; In Final Form: April 11, 2001

The kinetics and mechanism of the reactions OH + BrO → products (1) and OD + BrO → products (2) have been studied in the temperature ranges of 230−355 K and 230−320 K, respectively, and at total pressure of 1 Torr of helium using the discharge-flow mass spectrometric method. The following Arrhenius expressions for the total rate constants have been obtained from the kinetics of BrO consumption in excess of OH(OD) radical: $k_1 = (1.65 \pm 0.30) \times 10^{-11} \exp\{(250 \pm 50)/T\}$ cm^3 molecule^{-1} s^{-1} (with $k_1 = (3.8 \pm 0.9) \times 10^{-11}$ cm^3 molecule^{-1} s^{-1} at $T = 298$ K) and $k_2 = (1.7 \pm 0.6) \times 10^{-11} \exp\{(230 \pm 100)/T\}$ cm^3 molecule^{-1} s^{-1} (with $k_2 = (3.7 \pm 0.9) \times 10^{-11}$ cm^3 molecule^{-1} s^{-1} at $T = 298$ K), where uncertainties are twice the standard deviation. From the kinetics of HBr formation, the upper limit of the rate constant of the reaction OH + BrO → HBr + O_2 (1b) has been determined at $T = 298$ K: $k_{1b} < 1.0 \times 10^{-12}$ cm^3 molecule^{-1} s^{-1} ($k_{1b}/k_1 < 0.03$ for the branching ratio of channel 1b). Similarly, for the reaction OD + BrO → DBr + O_2 (2b), the rate constant at $T = 298$ K has been determined: $k_{2b} = (3.7 \pm 1.8) \times 10^{-13}$ cm^3 molecule^{-1} s^{-1} (which corresponds to the branching ratio $k_{2b}/k_2 = (1.0 \pm 0.5) \times 10^{-2}$). In addition, the rate constant of the reaction OD + DO_2 → D_2O + O_2 (3) has been measured for the first time: $k_3 = (3.8 \pm 0.9) \times 10^{-11}$ cm^3 molecule^{-1} s^{-1} at $T = 298$ K. This work suggests that the additional HBr source from the OH + BrO reaction, although significant, does not appear to be sufficient to explain the difference between current modeled and observed stratospheric HBr concentrations.

Introduction

The reaction between OH and BrO radicals may proceed following two channels:

$$OH + BrO \rightarrow Br + HO_2 \quad \Delta H = -(8.2 \pm 1.8) \text{ kcal mol}^{-1} \tag{1a}$$

$$\rightarrow HBr + O_2 \quad \Delta H = -(46.6 \pm 1.4) \text{ kcal mol}^{-1} \tag{1b}$$

(enthalpy data are from ref 1 except $\Delta H_{f,298}(HO_2) = 3.0 \pm 0.4$ kcal mol^{-1} [2,3] and $\Delta H_{f,298}(BrO) = 28.6 \pm 1.4$ kcal mol^{-1} [4]). Channel 1b is of potential importance for the stratospheric chemistry of bromine. One current issue in the bromine chemistry in the stratosphere is that models fail to reproduce (underestimate by a factor up to 6) the measured HBr concentration profiles. The existence of the minor HBr-forming pathway of reaction 1 may significantly influence the overall partitioning of bromine in the stratosphere, as well as the bromine-mediated ozone loss. It has been shown that a value of the branching ratio of as low as 1−2% for HBr formation in reaction 1 would reconcile model calculations[5,6] and stratospheric HBr measurements.[7] Thus, the determination of both the temperature dependence of the total rate constant and the branching ratio for the HBr-forming channel is of great importance. In the unique experimental study of the OH + BrO reaction,[8] only the room-temperature value of the overall rate constant has been measured with a large uncertainty: $k_1 = (7.5 \pm 4.2) \times 10^{-11}$ cm^3 molecule^{-1} s^{-1}.

The present work reports the results of the experimental study of reaction 1 at $T = 230$−355 K, including the measurement of the total rate constant and of the upper limit for the branching ratio of the HBr-forming channel. The detection of small yields of HBr from the OH + BrO reaction is an experimental problem, since significant residual concentrations of HBr are known to be present in the bromine-containing chemical systems used in the laboratory. In this respect, the reaction OD + BrO, which is the isotopic analogue of reaction 1, has been also studied in the present work, since it offers a more appropriate system for the determination of a low DBr yield compared to HBr yield in the OH + BrO system

$$OD + BrO \rightarrow Br + DO_2 \tag{2a}$$

$$\rightarrow DBr + O_2 \tag{2b}$$

In addition, the results of the measurements of the rate constant for the reaction between OD and DO_2 radicals, which is involved in the chemical system used for the determination of DBr yield in reaction 2, are also reported

$$OD + DO_2 \rightarrow D_2O + O_2 \tag{3}$$

Experimental Section

Experiments were carried out in a discharge flow reactor using a modulated molecular beam mass spectrometer as the detection method. The main reactor, shown in Figure 1 along with the triple movable injector for the reactants, consisted of a Pyrex tube (45 cm length and 2.4 cm i.d.) with a jacket for the thermostated liquid circulation (water or ethanol). The walls of the reactor as well as of the injector were coated with halocarbon

* Corresponding author. E-mail: bedjanian@cnrs-orleans.fr.
† Presently at CNRS - LPCE (Laboratoire de Physique et Chimie de l'Environnement), Orléans, France.

10.1021/jp010369q CCC: $20.00
Published on Web 06/01/2001

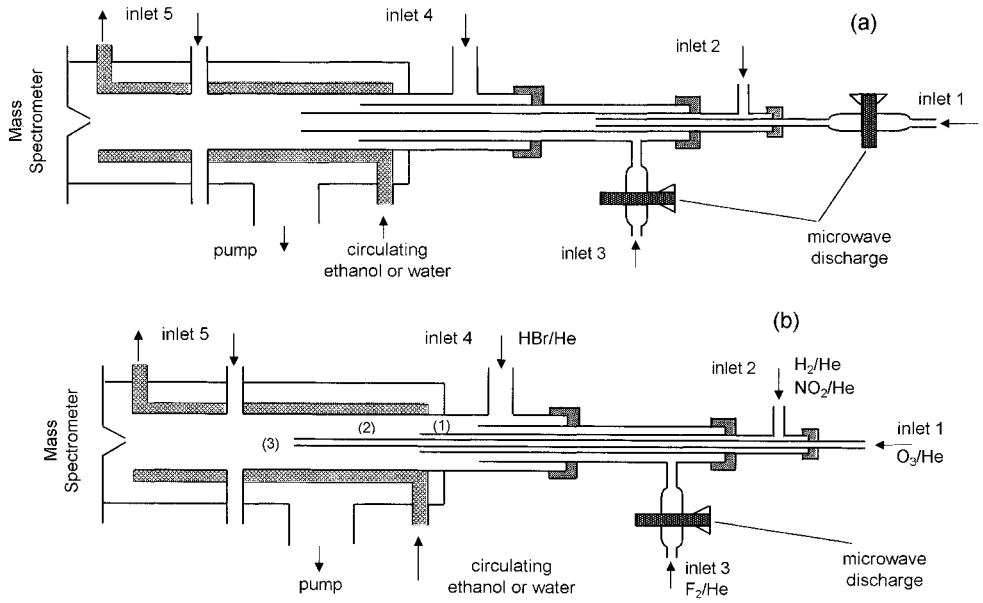

Figure 1. Diagram of the apparatus used in (a) the kinetic study of reactions 1 and 2 and (b) the mechanistic study of reactions 1 and 2.

wax in order to minimize the heterogeneous loss of active species. All experiments were conducted at 1 Torr total pressure, with helium as the carrier gas.

Two different methods were used for the generation of OH radicals. In the first one, the fast reaction of hydrogen atoms with NO_2 was used as the source of OH radicals

$$H + NO_2 \rightarrow OH + NO \quad (4)$$

$$k_4 = 4.0 \times 10^{-10} \exp(-340/T)\ \mathrm{cm^3\ molecule^{-1}\ s^{-1}}\ [1]$$

NO_2 was always used in excess over H atoms which were produced in a microwave discharge of H_2/He mixtures or in reaction 5

$$F + H_2 \rightarrow H + HF \quad (5)$$

$$k_5 = 1.4 \times 10^{-10} \exp(-500/T)\ \mathrm{cm^3\ molecule^{-1}\ s^{-1}}\ [1]$$

In the second method, OH radicals were produced in the reaction of F atoms with an excess of H_2O, with F atoms formed in the microwave discharge of F_2/He mixtures

$$F + H_2O \rightarrow OH + HF \quad (6)$$

$$k_6 = 1.4 \times 10^{-11} \exp\{(0 \pm 200)/T\}\ \mathrm{cm^3\ molecule^{-1}\ s^{-1}}\ [1]$$

To reduce F atom reactions with glass surface inside the microwave cavity, we inserted a ceramic (Al_2O_3) tube in this part of the injector. Similarly, the reaction of D atoms with excess NO_2 and reaction of F atoms with D_2O were used to form OD radicals

$$D + NO_2 \rightarrow OD + NO \quad (7)$$

$$k_7 = (1.20 \pm 0.25) \times 10^{-11}\ \mathrm{cm^3\ molecule^{-1}\ s^{-1}} \quad (T = 230-365\ \mathrm{K})\ [9]$$

$$F + D_2O \rightarrow OD + DF \quad (8)$$

$$k_8 = 8.4 \times 10^{-12} \exp(-260/T)\ \mathrm{cm^3\ molecule^{-1}\ s^{-1}}\ [10]$$

Deuterium atoms were formed in the microwave discharge of D_2 diluted in He or in the reaction of F atoms with D_2

$$F + D_2 \rightarrow D + DF \quad (9)$$

$$k_9 = 1.06 \times 10^{-10} \exp(-635/T)\ \mathrm{cm^3\ molecule^{-1}\ s^{-1}}\ [11]$$

OH and OD radicals were detected at their parent peaks at $m/e = 17$ (OH^+) and $m/e = 18$ (OD^+), respectively. These signals were corrected for contributions from H_2O and D_2O due to their fragmentation in the ion source (operated at 25−30 eV), the H_2O and D_2O being present in the reactor as precursors of the radicals and/or being formed in the reactions of disproportionation of OH and OD

$$OH + OH \rightarrow O + H_2O \quad (10)$$

$$k_{10} = 7.1 \times 10^{-13} \exp(210/T)\ \mathrm{cm^3\ molecule^{-1}\ s^{-1}}\ [9]$$

$$OD + OD \rightarrow O + D_2O \quad (11)$$

$$k_{11} = 2.5 \times 10^{-13} \exp(170/T)\ \mathrm{cm^3\ molecule^{-1}\ s^{-1}}\ [9]$$

These corrections could be easily done from the simultaneous detection of the signals of H_2O at $m/e = 17$ and 18 ($m/e = 18$ and 20 for D_2O). In another method, OH and OD radicals were detected as $HOBr^+$ ($m/e = 96/98$) and $DOBr^+$ ($m/e = 97/99$), respectively, after scavenging by an excess of Br_2 (added at the end of the reactor through inlet 5, located 5 cm upstream of the sampling cone) via reactions

$$OH + Br_2 \rightarrow Br + HOBr \quad (12)$$

$$k_{12} = 1.8 \times 10^{-11} \exp(235/T)\ \mathrm{cm^3\ molecule^{-1}\ s^{-1}}\ [12]$$

$$OD + Br_2 \rightarrow Br + DOBr \quad (13)$$

$$k_{13} = 1.9 \times 10^{-11} \exp(220/T)\ \mathrm{cm^3\ molecule^{-1}\ s^{-1}}\ [12]$$

This detection method did not require any corrections on the detected signals. The same procedure of OH(OD) chemical conversion to HOBr(DOBr) was used for the measurements of the absolute concentrations of these radicals: [OH] = [HOBr]

$= \Delta[Br_2]$ ($[OD] = [DOBr] = \Delta[Br_2]$). Thus, OH and OD concentrations were determined from the consumed fraction of $[Br_2]$. This method allowed also for the determination of the absolute concentrations of HOBr and DOBr. $[Br_2]$ was determined from the measured flow rate of known Br_2/He mixtures. The possible influence of secondary chemistry on this detection method and on the OH(OD) calibration procedure was discussed in details in previous papers.[9,12]

Two reactions were used to produce BrO radicals

$$O + Br_2 \rightarrow BrO + Br \quad (14)$$

$$k_{14} = 1.8 \times 10^{-11} \exp(40/T)\ cm^3\ molecule^{-1}\ s^{-1}\ [13]$$

$$Br + O_3 \rightarrow BrO + O_2 \quad (15)$$

$$k_{15} = 1.7 \times 10^{-11} \exp(-800/T)\ cm^3\ molecule^{-1}\ s^{-1}\ [1]$$

O atoms were generated from the microwave discharge in O_2/He mixtures. Br atoms were produced either from the microwave discharge of Br_2/He mixtures or in reaction 16 between F atoms and HBr (for the mechanistic study of reactions 1 and 2)

$$F + HBr \rightarrow Br + HF \quad (16)$$

$$k_{16} = 2.5 \times 10^{-10} \exp(-506/T)\ cm^3\ molecule^{-1}\ s^{-1}\ [14]$$

BrO radicals were detected at their parent peak at $m/e = 95/97$ as BrO^+. Two methods have been used for the determination of the absolute concentrations of BrO radicals. The first one consisted of the usual procedure of BrO titration with NO, with the subsequent detection of NO_2 formed ($[BrO] = [NO_2]$)

$$BrO + NO \rightarrow Br + NO_2 \quad (17)$$

$$k_{17} = 8.8 \times 10^{-12} \exp(260/T)\ cm^3\ molecule^{-1}\ s^{-1}\ [1]$$

In this case, BrO was formed in reaction 14 in order to avoid the regeneration of BrO through reaction 15 when O_3 was present in the reactor. Another method for the calibration of BrO signals employed reaction 15 between Br atoms and ozone. Br atoms, formed in the microwave discharge of Br_2, were consumed by using high ozone concentrations ($[O_3] \approx 10^{15}$ molecules cm^{-3}). The concentration of BrO was then determined from the fraction of Br_2 dissociated in the microwave discharge. In these calibration experiments, the influence of the recombination reaction of BrO radicals (eq 18) (leading to steady state for Br) was negligible due to the high ozone concentrations used

$$BrO + BrO \rightarrow Br + Br + O_2 \quad (18a)$$

$$\rightarrow Br_2 + O_2 \quad (18b)$$

$$k_{18a} = 2.4 \times 10^{-12} \exp(40/T)\ cm^3\ molecule^{-1}\ s^{-1}\ [1]$$

$$k_{18b} = 2.8 \times 10^{-14} \exp(860/T)\ cm^3\ molecule^{-1}\ s^{-1}\ [1]$$

Besides, all bromine containing species involved in reactions 15 and 18 were detected, and the small concentrations of Br atoms (not transformed to BrO) could be easily taken into account: $2\Delta[Br_2] = [BrO] + [Br]$, where $\Delta[Br_2]$ is the fraction of Br_2 dissociated in the discharge. The absolute concentrations of BrO determined by these different methods were always in good agreement (within a few percent).

HO_2 radicals, Br atoms, and HBr molecules were observed in the chemical system used for the determination of the branching ratio for the channel (1b) of reaction 1. For the determination of the absolute concentrations of HO_2, the fast reaction of fluorine atoms with H_2O_2 was used as the source of HO_2 radicals, with F atoms produced in microwave discharge of F_2/He mixtures

$$F + H_2O_2 \rightarrow HO_2 + HF \quad (19)$$

$$k_{19} = 5.0 \times 10^{-11}\ cm^3\ molecule^{-1}\ s^{-1}\ (T = 300\ K)\ [15]$$

It was verified by mass spectrometry that more than 90% of F_2 was dissociated in the microwave discharge. H_2O_2 was always used in excess over F atoms. Absolute concentrations of HO_2 were measured using chemical conversion of HO_2 to NO_2 through reaction 20

$$HO_2 + NO \rightarrow OH + NO_2 \quad (20)$$

$$k_{20} = 3.5 \times 10^{-12} \exp(250/T)\ cm^3\ molecule^{-1}\ s^{-1}\ [1]$$

This reaction leads to the simultaneous production of OH radicals. To prevent the possible HO_2 regeneration by reaction 21, we carried out calibration experiments in the presence of Br_2 in the reactor

$$OH + H_2O_2 \rightarrow HO_2 + H_2O \quad (21)$$

$$k_{21} = 2.9 \times 10^{-12} \exp(-160/T\}\ cm^3\ molecule^{-1}\ s^{-1}\ [1]$$

Thus, OH was rapidly consumed by Br_2 through reaction 12. Similarly, reaction 22 of F atoms with D_2O_2 was used to produce DO_2 radicals and reaction 23 to measure their absolute concentrations

$$F + D_2O_2 \rightarrow DO_2 + DF \quad (22)$$

$$DO_2 + NO \rightarrow OD + NO_2 \quad (23)$$

$$k_{23} = (1.1 \pm 0.3) \times 10^{-11}\ cm^3\ molecule^{-1}\ s^{-1}\ (T = 297K)\ [16]$$

The concentrations of NO_2 and of the other stable species used were determined from the measurements of pressure drop rate in flasks containing mixtures of known dilution. The HO_2 and DO_2 radicals were detected at their parent peaks at $m/e = 33$ (HO_2+) and $m/e = 34$ (DO_2+), respectively. These signals were always corrected for contributions from H_2O_2 and D_2O_2 due to their fragmentation in the ion source. These corrections were made from the simultaneous detection of the signals from H_2O_2 at $m/e = 33$ and 34 ($m/e = 34$ and 36 for D_2O_2), respectively.

Bromine atoms were detected at their parent peaks as Br^+ ($m/e = 79/81$). The absolute concentrations of Br atoms could be obtained from the fraction of Br_2 dissociated in the microwave discharge ($[Br] = 2\Delta[Br_2]$).

The absolute calibration of HBr (detected at its parent peaks $m/e = 80/82$) was obtained from the flow rate measurements of known HBr/He mixtures. This method had to be applied with special care, since it is known that HBr can decompose during its storage, giving H_2 and Br_2. In the present study, HBr (Aldrich, stated purity > 99.8%) was purified by distillation before use. HBr/He mixtures were stored in a glass flask which was previously passivated with HBr. It was verified by mass spectrometry (detection of the possible decomposition product Br_2 and invariance of the HBr calibration from day to day) that no significant decomposition of HBr occurred during its storage for a few weeks. The decomposition product, Br_2, was measured to be less than 0.1% of HBr. To verify the reliability of these

measurements of the HBr absolute concentrations, we used another method. It consisted of the chemical conversion of HBr to Br by an excess of F atoms through reaction 16. In this case, the concentration of HBr could be related to the concentration of the Br atoms formed. The relation between HBr and Br signals obtained by this method was in good agreement (within a few percent) with the results of the independent calibrations of HBr and Br. In the experiments with DBr detection, the calibration factor (concentration-to-signal ratio) was considered to be the same for HBr and DBr ($m/e = 81/83$). This hypothesis was verified experimentally. Using the chemical conversion of H and D atoms to HBr and DBr via reactions 24 and 25, respectively, we could relate the intensity of both HBr and DBr signals the concentration of Br_2

$$H + Br_2 \rightarrow Br + HBr \quad (24)$$

$$k_{24} = 6.7 \times 10^{-10} \exp(-673/T)\ \mathrm{cm^3\ molecule^{-1}\ s^{-1}}\ [17]$$

$$D + Br_2 \rightarrow Br + DBr \quad (25)$$

$$k_{25} = 6.0 \times 10^{-10} \exp(-709/T)\ \mathrm{cm^3\ molecule^{-1}\ s^{-1}}\ [17]$$

In these experiments, the ratio of concentration to signal intensity was found to be the same for HBr and DBr.

Ozone was produced by an ozonizer (Trailigaz) and was collected and stored in a trap containing silica gel at $T = 195$ K. The trap was pumped before use in order to reduce the O_2 concentration. The resulting oxygen concentration was always less than 20% of the ozone concentration introduced into the reactor. The absolute concentration of O_3 was derived using the reaction of ozone and NO with simultaneous detection of ozone consumed and NO_2 formed ($\Delta[O_3] = \Delta[NO_2]$)

$$NO + O_3 \rightarrow NO_2 + O_2 \quad (26)$$

$$k_{26} = 2.0 \times 10^{-12} \exp(-1400/T)\ \mathrm{cm^3\ molecule^{-1}\ s^{-1}}\ [1]$$

The purities of the gases used were as follows: He, >99.9995% (Alphagaz) was passed through liquid nitrogen traps; O_2 > 99.995% (Alphagaz); H_2 > 99.998% (Alphagaz); D_2 > 99.7% (Alphagaz); D_2O (99.9% D, Euriso-top); $H_2{}^{18}O$ (96.5% ^{18}O, Euriso-top); Br_2 > 99.99% (Aldrich); F_2 (5% in Helium, Alphagaz); NO_2 > 99% (Alphagaz); NO, >99% (Alphagaz), was purified by trap-to trap distillation in order to remove NO_2 traces. A 70% H_2O_2 solution was purified to around 90% by flowing helium through the bubbler containing H_2O_2.

Results

1. Reaction OH + BrO → Products. The determination of the total rate constant for reaction 1 represents a significant experimental challenge, as it is difficult to avoid the influence of multiple possible secondary and side processes involving reactants and products of reaction 1 as well as the precursors of OH and BrO radicals. In the present work, two different approaches were used to measure the rate constant of reaction 1. First, k_1 was measured directly under pseudo-first-order conditions using an excess of OH over BrO radicals. In another series of experiments, a relative rate method was employed, using the reaction OH + Br_2 as the reference.

a. Absolute Measurements of the Total Rate Constant. In this series of experiments, the rate constant of reaction 1 was derived from the kinetics of BrO consumption monitored in excess of OH radicals. The configuration used for the introduction of the reactants into the reactor is shown in Figure 1a. OH radicals were formed either in the reaction of H atoms with NO_2 or in the reaction of F atoms with H_2O. H or F atoms formed in the microwave discharge (inlet 3) were introduced into the reactor through the outer tube of the movable injector, and NO_2 or H_2O was passed through the reactor sidearm (inlet 4). The second reactant, BrO radicals, was formed in the central tube of the sliding injector through the reaction of oxygen atoms (inlet 1) with excess Br_2 (inlet 2). Concentrations of the reactant precursors, Br_2 and NO_2, in the reactor were $0.5-1.0 \times 10^{12}$ and $6-7 \times 10^{13}$ molecules cm^{-3}, respectively. NO was another species present in the reactor, since it was formed in the OH source (reaction 4) and in the sequence of reactions 10 and 27

$$OH + OH \rightarrow O + H_2O \quad (10)$$

$$O + NO_2 \rightarrow NO + O_2 \quad (27)$$

$$k_{27} = 6.5 \times 10^{-12} \exp(120/T)\ \mathrm{cm^3\ molecule^{-1}\ s^{-1}}\ [1]$$

NO thus formed ($[NO] \geq [OH]_0$) led to additional BrO consumption in reaction 17

$$BrO + NO \rightarrow Br + NO_2 \quad (17)$$

The F + H_2O reaction is NO_x free source of OH radicals. However, in absence of NO_2 in reactor, the O atoms formed in reaction 10 and, to a lesser extent, through reaction 28 in the OH production zone

$$F + OH \rightarrow O + HF \quad (28)$$

can further react. Under the present experimental conditions, oxygen atoms could lead either to the generation of BrO radicals in reaction 14 with Br_2 or to the consumption of BrO in reaction 29

$$O + BrO \rightarrow Br + O_2 \quad (29)$$

$$k_{29} = 1.9 \times 10^{-11} \exp(230/T)\ \mathrm{cm^3\ molecule^{-1}\ s^{-1}}\ [1]$$

For this reason, in the experiments using F + H_2O reaction to produce OH radicals, NO_2 was also introduced into the reactor (inlet 4) in order to scavenge the O atoms. Thus, NO was always present in the reactor, and the measurements of the rate constant of reaction 1 were conducted in the presence of NO. The range of the initial concentrations of OH is shown in Table 1, whereas

TABLE 1: Reaction OH + BrO → Products (1): Experimental Conditions and Results for the Direct Measurements of the Rate Constant

T (K)	no/exp.[a]	$[OH]_0$[b]	source of OH	detection of OH[c]	k_1[d]
355	8	0.6−7.3	H + NO_2	OH^+	3.3 ± 0.8
323	6	0.7−6.7	H + NO_2	OH^+	3.4 ± 0.9
320	8	0.6−8.0	H + NO_2	$HOBr^+$	4.0 ± 1.0
320	7	0.7−7.4	F + H_2O	$HOBr^+$	3.5 ± 0.9
300	22	0.8−10.3	H + NO_2	$HOBr^+$	3.6 ± 0.9
298	9	0.7−7.2	F + H_2O	$HOBr^+$	3.9 ± 1.0
273	8	0.6−7.2	H + NO_2	$HOBr^+$	4.3 ± 1.1
270	8	0.8−6.4	F + H_2O	$HOBr^+$	4.0 ± 1.0
250	7	0.7−9.0	H + NO_2	$HOBr^+$	4.3 ± 1.1
248	8	0.7−7.2	F + H_2O	$HOBr^+$	4.6 ± 1.2
230	8	0.6−5.8	H + NO_2	OH^+	4.9 ± 1.2

[a] Number of kinetic runs. [b] Concentrations are in 10^{12} molecules cm^{-3}. [c] OH radicals were detected as OH^+ ($m/e = 17$) or as $HOBr^+$ ($m/e = 96/98$) after scavenging by excess Br_2 (see text). [d] Rate constants are in 10^{-11} cm^3 $molecule^{-1}$ s^{-1}, and errors are the conservative 25% uncertainties, including estimated systematic errors.

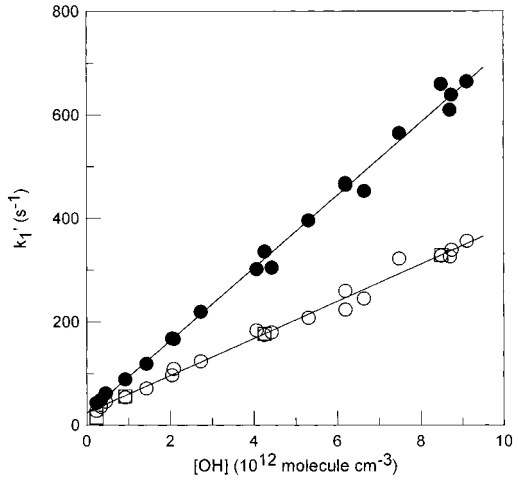

Figure 2. Example of pseudo-first-order plot of BrO consumption in the reaction with excess OH radicals in the presence of NO: OH source is the reaction H + NO_2, $T = 300$ K, $k_1'_{measured} = k_1[OH] + k_{17}[NO] + k_w$ (filled circles),$k_1' = k_1[OH] + k_w$ (open circles; see text), and the pseudo-first-order plot of Br_2 consumption in the reaction with OH (squares).

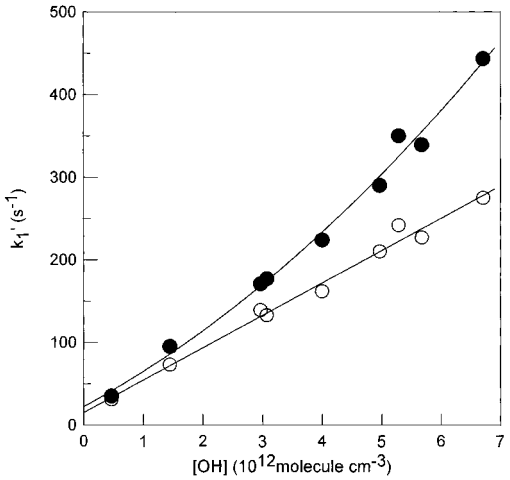

Figure 3. Example of pseudo-first-order plot of BrO consumption in the reaction with excess OH radicals in the presence of NO: OH source is the reaction F + H_2O, $T = 298$ K, $k_1'_{measured} = k_1[OH] + k_{17}[NO] + k_w$ (filled circles), and $k_1' = k_1[OH] + k_w$ (open circles; see text).

the initial concentration of BrO radicals was $(1.5-2.0) \times 10^{11}$ molecules cm^{-3}. The linear flow velocity in the reactor was in the range of 1600−2200 cm s^{-1}.

The observed consumption of BrO was due to reaction 1, reaction 17, and wall loss (k_w). The reaction of BrO with HO_2, which is the main product of reaction 1, had negligible impact on the kinetics of BrO due to the low initial concentrations of BrO and the occurrence of the fast reaction of HO_2 with OH

$$BrO + HO_2 \rightarrow HOBr + O_2 \qquad (30)$$

$$k_{30} = 9.4 \times 10^{-12} \exp(345/T)\ cm^3\ molecule^{-1}\ s^{-1}\ [18]$$

$$OH + HO_2 \rightarrow H_2O + O_2 \qquad (31)$$

$$k_{31} = 4.8 \times 10^{-11} \exp(250/T)\ cm^3\ molecule^{-1}\ s^{-1}\ [1]$$

Thus, the pseudo-first-order rate constant which could be derived from the exponential fit to the experimental BrO decays was

$$k_1'_{measured} = k_1[OH] + k_{17}[NO] + k_w$$

When the known value of k_{17} and the concentration of NO in the reactor (which was directly measured by mass spectrometry) were considered, the contribution of reaction 17 could be easily calculated and extracted from $k_1'_{measured}$ to obtain the corrected value $k_1' = k_1[OH] + k_w$. An example of the dependencies of the measured and corrected pseudo-first-order rate constants versus OH concentration (with reaction 4 as a source of OH) is shown in Figure 2. The correction on $k_1'_{measured}$ due to the reaction of BrO with NO is around 50% in this case. The rate constant of reaction 1 was calculated from the slope of the linear fit of the plots of the corrected pseudo-first-order rate constant versus OH concentration. All the values of $k_1'_{measured}$ were corrected also for axial and radial diffusion[19] of BrO. The diffusion coefficient D_{BrO-He} was calculated from D_{Kr-He}.[20] Typical corrections were within 10%. A similar example, obtained with reaction 6 as a source of OH, is shown in Figure 3. One can note that in this case, the correction on $k_1'_{measured}$ is higher at the highest concentrations of OH. This could be expected since the main source of NO in this case is reaction 27 of NO_2 with O, the oxygen atoms being formed in the OH + OH reaction. One can also note that the corrected k_1' data are well fitted by the linear dependence versus [OH], which is not the case for the measured values of the pseudo-first order rate constant. This seems to show that the contribution of the BrO + NO side reaction to the consumption of BrO is properly taken into account by the applied procedure. A consumption of the excess reactant, OH radicals, was also observed (generally lower than 20%, however, up to 50% in a few kinetic runs). This OH consumption was due to reaction with BrO (eq 1), HO_2 (eq 31), and Br_2 (eq 12) to the OH disproportionation reaction 10, to reaction with NO_2 (eq 32), and to the heterogeneous loss of OH

$$OH + NO_2\ (+M) \rightarrow HNO_3\ (+M) \qquad (32)$$

$$k_{32} = 2.5 \times 10^{-30}(T/300)^{-4.4}\ cm^6\ molecule^{-2}\ s^{-1}\ (\text{for M} = N_2)\ [1]$$

This value of k_{32} is recommended in ref 1 for M = N_2. The value of k_{32} with He as a third body can be lower by a factor 2−3.[21] By comparison, the rate constants of the reaction of OD with NO_2 reported in ref 22 are $k = 4.05 \times 10^{-30}$ and 1.27×10^{-30} cm^6 $molecule^{-2}$ s^{-1} for M = N_2 and He, respectively. In the calculation of the rate constants, [OH] and [OD] have been kept constant, with a mean value along the BrO decay kinetics. A numerical simulation of the BrO decay kinetics, using the observed [OH] temporal profiles, gave the same values for k_1 (within 5%). The final results obtained for k_1 in this series of experiments are given in Table 1 and are also presented in Figure 4. A good agreement can be noted for the results obtained for k_1 under the different experimental conditions and with the different methods for the OH detection. The uncertainties on k_1 represent 25% conservative uncertainty, which is the combination of statistical and estimated systematic errors. The estimated systematic uncertainties include ±5% for flow meter calibrations, ±1% for temperature, ±3% for pressure, and ±10% for the absolute OH concentrations. Combining these uncertainties in quadrature and adding ∼15% for the statistical error and uncertainty on the contribution of BrO + NO reaction yield ∼25% overall uncertainty on the values of k_1.

Possible error from the method of OH detection as $HOBr^+$ (m/e = 96/98) has been considered. Additional HOBr could be formed in the main reactor as a result of the secondary reaction

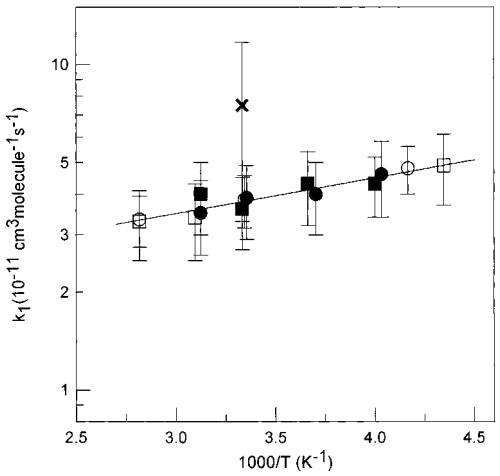

Figure 4. Temperature dependence of the total rate constant of the reaction OH + BrO → products (1): (●) OH source is the reaction F + H_2O, with OH detected as $HOBr^+$; (■) OH source is the reaction H + NO_2, with OH detected as $HOBr^+$; (□) OH source is the reaction H + NO_2, with OH detected as OH^+; (○) relative measurements of k_1; (×) data from ref 8.

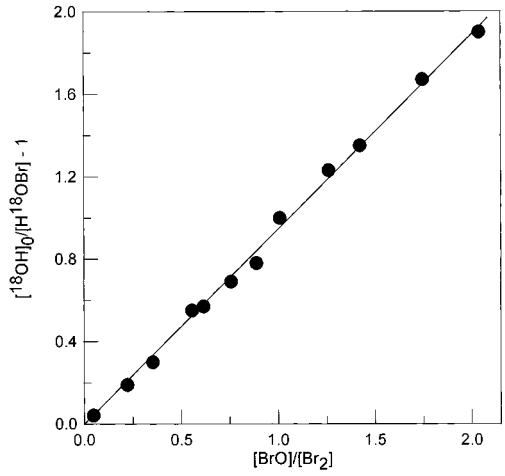

Figure 5. Reaction OH + BrO → products (1): relative measurements of the rate constant (see text).

of BrO with HO_2 (30) (produced in reaction 1) and reaction 12 of OH with Br_2 from BrO source. This could lead to the overestimation of the OH concentration in the reactor. However, this HOBr formed in the reaction system could be easily observed (when Br_2 was not added at the end of the reactor) and could be extracted from the HOBr signal corresponding to the concentration of OH (measured with addition of Br_2 at the end of the reactor). The concentration of HOBr from reactions 12 and 30 was always much lower than that corresponding to the OH concentration.

b. Relative Measurements of the Rate Constant. In this series of experiments, the rate constant of reaction 1 was measured using the reaction of OH with Br_2 as the reference

$$OH + Br_2 \rightarrow HOBr + Br \qquad (12)$$

The temperature dependence of the rate constant of this reaction is well established, considering the excellent agreement between two recent measurements: $k_{12} = (1.98 \pm 0.51) \times 10^{-11}$ exp $[(238 \pm 70)/T]$[23] and $k_{12} = (1.8 \pm 0.3) \times 10^{-11}$ exp $[(235 \pm 50)/T]$ cm^3 molecule^{-1} s^{-1}.[12] The approach used in this relative study consisted of the titration of the initial concentration of OH, $[OH]_0$, by a mixture of excess BrO and Br_2 and the measurements of the HOBr yield as a function of the [BrO]/[Br_2] ratio. The concentration of HOBr formed is simply defined by the fraction of $[OH]_0$ reacting with Br_2

$$[HOBr] = \frac{k_{12}[Br_2]}{k_{12}[Br_2] + k_1[BrO]}[OH]_0 \qquad (I)$$

Considering the derived expression

$$\frac{[OH]_0}{[HOBr]} - 1 = \frac{k_1}{k_{12}} \times \frac{[BrO]}{[Br_2]} \qquad (II)$$

we can obtain the rate constant ratio k_1/k_{12} and, hence, k_1 by plotting $[OH]_0/[HOBr] - 1$ as a function of the [BrO]/[Br_2] ratio. The main experimental difficulty in these measurements is that additional HOBr can be formed in the fast secondary reaction of BrO with HO_2 (30), the HO_2 being produced in reaction 1. To exclude this possibility, we carried out all the experiments described below using isotopically labeled OH radicals, ^{18}OH. In this case, the reaction $^{18}OH + Br_2$ produces $H^{18}OBr$, whereas the sequence of reactions 1a and 30 leads to $H^{16}OBr$ formation

$$^{18}OH + Br^{16}O \rightarrow H^{18}O^{16}O + Br \qquad (1a)$$

$$Br^{16}O + H^{18}O^{16}O \rightarrow H^{16}OBr + {}^{18}O^{16}O \qquad (30)$$

Thus, the primary and secondary sources of HOBr can be distinguished.

In these experiments, ^{18}OH radicals were produced via the reaction of F atoms with $H_2{}^{18}O$ and were introduced into the reactor through the central tube of the movable injector. The BrO/Br_2 mixture was prepared by reaction of oxygen atoms (microwave discharge of O_2/He, inlet 3) with excess Br_2 (inlet 4) through reaction 14. To reach higher concentrations of BrO and to minimize the BrO + BrO reaction, we added ozone into the reactor

$$Br + O_3 \rightarrow BrO + O_2 \qquad (15)$$

Both BrO and Br_2 concentrations were varied, and the yield of $H^{18}OBr$ (detected at $m/e = 100$) was measured as a function of [BrO]/[Br_2] ratio. A typical experimental plot, measured at $T = 240$ K, is shown in Figure 5. According to expression II, the slope of this linear dependence gives the k_1/k_{12} ratio. All the results obtained at three temperatures ($T = 355$, 299, and 240 K) are presented in Table 2, which also reports the initial concentrations of ^{18}OH, Br_2, and BrO used as well as the final results obtained for k_1. The values of k_{12} used in the calculations of k_1 were determined from the Arrhenius expression $k_{12} = 1.9 \times 10^{-11}$ exp$(235/T)$ cm^3 molecule^{-1} s^{-1} (preexponential factor is the mean of those reported in refs 12 and 23) with the addition of a conservative 15% uncertainty, considering that in refs 12 and 23 (i) similar values were measured for the activation factor, $E/R = 238$ and 235 K, respectively, and (ii) the difference between the reported preexponential factors was around 10%.

One of the advantages of the above approach for the determination of k_1/k_{12} ratio is that it does not require measurements of the absolute concentrations of the involved species. $[OH]_0$ could be expressed in the relative units as HOBr signal when $[OH]_0$ was titrated by an excess of Br_2. Thus, in these experiments, only HOBr signal was detected, first in the absence of BrO (corresponding to $[OH]_0$) and second in the presence of

TABLE 2: Reaction OH + BrO → Products (1): Experimental Conditions and Results for the Relative Measurements of the Rate Constant

T (K)	$[OH]_0$[a]	[BrO][b]	$[Br_2]$[b]	$[BrO]/[Br_2]$	k_1/k_{12}[c]	k_1[d]
355	3.0	1.0−4.2	2.0−9.2	0.11−1.57	0.91 ± 0.02	3.35 ± 0.60
299	2.5	1.1−4.4	2.6−7.8	0.15−1.45	0.92 ± 0.03	3.85 ± 0.70
240	2.3−6.4	0.3−4.0	1.9−7.0	0.05−2.04	0.95 ± 0.02	4.8 ± 0.8

[a] Concentrations are in 10^{11} molecules cm^{-3}. [b] Concentrations are in 10^{13} molecules cm^{-3}. [c] Uncertainty of the k_1/k_{12} ratio is 1σ from the linear fit. [d] Rate constants are in 10^{-11} cm^3 molecule^{-1} s^{-1}, and uncertainty of k_1 represents combination of the uncertainties of k_{12} (15%) and k_1/k_{12} (1σ).

BrO/Br_2 (corresponding to the fraction of $[OH]_0$ reacted with Br_2). The measurements of the absolute concentrations of BrO and Br_2 could be also avoided, since the mass spectrometric signals of these species could be related to each other using the reaction of excess ozone with Br atoms from the microwave discharge of Br_2. In this case, $2\Delta[Br_2] = [BrO]$, and one can easily find the relation between the signals of BrO and Br_2, which correspond to the same concentrations of these species. This relative calibration was verified to be in good agreement with the absolute measurements of Br_2 and BrO concentrations (as described in Experimental Section).

The possible influence of secondary chemistry on the obtained results appears to be negligible. There are two important assumptions for the above treatment to be correct: (i) OH is only consumed in reactions with BrO and Br_2, and (ii) no other sources of $H^{18}OBr$ than reaction 12 exist. These conditions were satisfied due to (i) the use of low initial concentrations of OH and high concentrations of BrO and Br_2 (to ensure negligible contribution of OH + OH and OH + O_3 reactions) and (ii) the use of isotopically labeled OH.

The results of another approach in this relative study of reaction 1 are shown in Figure 2. In this case, the kinetics of Br_2 (Br_2 from the source of BrO) and BrO in their reaction with OH radicals were observed simultaneously. As one can see from the data presented in Figure 2, similar values for the pseudo-first-order rate constants were observed from BrO and Br_2 decays, indicating that the ratio k_1/k_{12} is around unity at T = 300 K.

The results of the relative measurements of k_1 are in excellent agreement with those from the absolute study (Tables 1 and 2). The temperature dependence of k_1, combining all the data obtained for k_1, is presented in Figure 4. The following Arrhenius expression is derived:

$$k_1 = (1.65 \pm 0.30) \times 10^{-11} \exp[(250 \pm 50)/T] \text{ cm}^3 \text{ molecule}^{-1} \text{ s}^{-1} \qquad T = (230-355) \text{ K}$$

Quoted uncertainties represent two standard deviations.

c. Measurements of the Branching Ratio for the HBr-Forming Channel OH + BrO → HBr + O_2 (1b). The determination of an expected low branching ratio for the HBr-forming channel of reaction 1 is an experimental challenge since (i) small amounts of the minor product, HBr, should be detected and quantified and (ii) relatively high background concentrations of HBr are known to be always present in the reactor when Br containing species are used and, particularly, when a microwave discharge of Br_2 is operated. Considering this, we conducted the experiments with relatively high concentrations of the reactants, OH and BrO. The disadvantage of such experimental conditions is that secondary reactions cannot be avoided and can significantly affect the quantitative detection of the minor product. In the present study, this problem has been solved by observing directly the kinetics of all the species (reactants, intermediates) involved in HBr formation and consumption.

TABLE 3: Measurements of the Rate Constant of the Reaction OH + BrO → HBr + O_2 (1b): Mechanism Used in the Computer Simulations

reaction	rate constant[a]
OH + BrO → HBr + O_2	k_{1b}, varied
OH + BrO → Br + HO_2	k_{1a}, varied
OH + HO_2 → H_2O + O_2	1.1×10^{-10}
HO_2 + BrO → HOBr + O_2	3.1×10^{-11}
HO_2 + Br → HBr + O_2	1.7×10^{-12}
HO_2 + NO → OH + NO_2	8.1×10^{-12}
HO_2 + O_3 → OH + $2O_2$	2.0×10^{-15}
BrO + NO → Br + NO_2	2.1×10^{-11}
BrO + BrO → Br + Br + O_2	2.7×10^{-12}
BrO + BrO → Br_2 + O_2	0.5×10^{-12}
Br + O_3 → BrO + O_2	1.2×10^{-12}
OH + O_3 → HO_2 + O_2	6.8×10^{-14}
OH + HBr → Br + H_2O	1.1×10^{-11}
OH + OH → O + H_2O	1.4×10^{-12}
O + OH → H + O_2	3.3×10^{-11}
O + HO_2 → OH + O_2	5.9×10^{-11}
O + BrO → Br + O_2	4.1×10^{-11}
O + NO_2 → NO + O_2	9.7×10^{-12}
H + O_3 → OH + O_2	2.9×10^{-11}
H + NO_2 → OH + NO	1.3×10^{-10}
NO + O_3 → NO_2 + O_2	1.8×10^{-14}
BrO + wall → loss	3 s^{-1}
OH + wall → loss	5 s^{-1}
HO_2 + wall → loss	5 s^{-1}

[a] For bimolecular reactions, units are cm^3 molecule^{-1} s^{-1}; all rate constants at T = 298 K are from ref 1, except HO_2 + BrO,[18] HO_2 + Br,[24] OH + OH,[9] OH + HBr,[25] and the wall loss rates measured in this work.

Experiments were carried out at 1 Torr total pressure and only at room temperature. The configuration of the flow system used in these experiments is shown in Figure 1b. The initial reactants, OH and BrO, were formed in a sequence of reactions conducted in different regions of the main reactor. In region 1, HBr molecules were transformed into Br atoms by fast reaction with an excess of atomic fluorine (from microwave discharge of F_2/He mixtures). Further, H_2/NO_2 mixture was added to this chemical system. In reaction zone 2, F atoms were completely consumed by an excess of H_2, and hydrogen atoms thus formed reacted with NO_2, producing OH radicals. Finally, in region 3, i.e., in the main reactor, Br atoms reacted with ozone to form BrO radicals. This configuration allowed (i) a Br_2 free chemical system (to avoid the fast side reaction OH + Br_2) with relatively high concentrations of the reactants, OH and BrO (up to 10^{13} molecules cm^{-3}), and (ii) avoiding the use of the microwave discharge of Br_2, which should have led to high background concentrations of HBr. The kinetics for eight species involved in this complicated chemical system were observed: OH, BrO, Br, HO_2, NO, NO_2, HOBr, and HBr. A reaction mechanism used in the simulation of the experimental curves is shown in Table 3. An example of the experimental and simulated kinetics is presented in Figure 6. The variable parameters were the rate constants of reactions 1a and 1b. They were determined from the best fit to the kinetics of OH consumption and HBr formation, respectively. For all other species, a good agreement

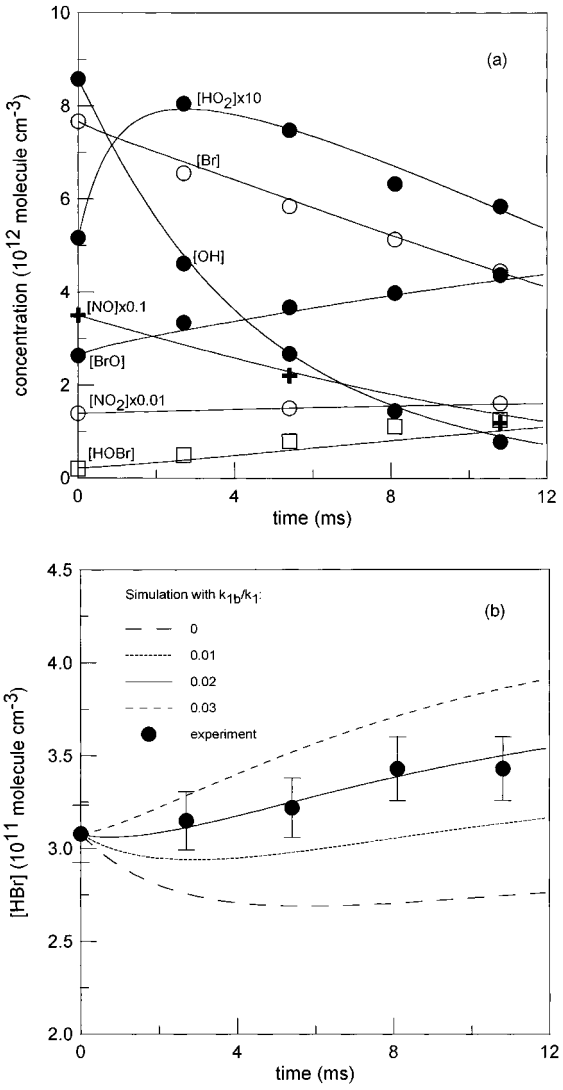

Figure 6. Example of experimental (points) and simulated (lines) kinetics for the species detected in the chemical system used for the study of the reaction OH + BrO → HBr + O_2 (1b): $t = 0$ corresponds to the first observation point at the top of the reaction zone (see text for Figure 6a,b).

(typically within 10%) between experimental data and results of the simulation was achieved without any variation of the kinetic parameters. Although the reaction mechanism used in the simulation of the experimental data appears to be rather complex, the kinetics of HBr is, in fact, defined by only three processes: reactions 1b and 33, leading to HBr formation, and reaction 34, leading to HBr consumption

$$HO_2 + Br \rightarrow HBr + O_2 \quad (33)$$

$$k_{33} = 4.9 \times 10^{-12} \exp(-310/T)\ \text{cm}^3\ \text{molecule}^{-1}\ \text{s}^{-1}\ [24]$$

$$OH + HBr \rightarrow Br + H_2O \quad (34)$$

$$k_{34} = 5.3 \times 10^{-12} \exp(225/T)\ \text{cm}^3\ \text{molecule}^{-1}\ \text{s}^{-1}\ [25]$$

Thus, the simulated profiles of HBr are only sensitive to the rate constants for reactions 1b, 33, and 34 and to the concentration profiles of OH, BrO, Br, and HO_2. All these species were directly detected and their absolute concentrations were measured. From Figure 6a, it can be seen that the reaction mechanism used for the simulation gives an adequate representation of the chemical processes occurring in the reactor. Figure 6b shows the sensitivity of the HBr profiles to the rate constant of reaction 1b (presented as the branching ratio k_{1b}/k_1 with $k_1 = 3.8 \times 10^{-11}$ cm^3 molecule^{-1} s^{-1} from this work). All the results obtained for k_{1a} and k_{1b} in a series of five experiments are shown in Table 4. One can note that the results obtained for the total rate constant of reaction 1, $k_1 = k_{1a} + k_{1b}$, are in excellent agreement with those obtained in the kinetic study of the reaction, although they were determined under completely different experimental conditions. The mean value for k_{1b} from this series of experiments is $k_{1b} = (6.7 \pm 1.9) \times 10^{-13}$ cm^3 molecule^{-1} s^{-1} (where uncertainty represents 95% confidence limits on the results of the simulation). Using the value of $k_1 = (3.8 \pm 0.9) \times 10^{-11}$ cm^3 molecule^{-1} s^{-1}, we find the branching ratio of the channel (1b) to be $k_{1b}/k_1 = (1.8 \pm 0.8) \times 10^{-2}$.

TABLE 4: Measurements of the Rate Constant for the Reaction OH + BrO → HBr + O_2 (1b): Experimental Conditions and Results

no	[OH]^a	[BrO]^a	$k_{1a}/10^{-11}$ ^{b}	$k_{1b}/10^{-13}$ ^{b}
1	7.3	4.6	3.7 ± 0.2	6.7 ± 1.0
2	7.8	4.3	3.6 ± 1.0	6.6 ± 1.0
3	8.2	6.3	3.5 ± 0.5	4.2 ± 1.2
4	8.6	2.6	3.7 ± 0.3	7.4 ± 0.6
5	9.2	3.0	3.6 ± 0.4	8.4 ± 1.4

^{a} Concentrations are in 10^{12} molecules cm^{-3}, and the concentrations represent those measured at the top of the reaction zone; ^{b} Rate constants are in cm^3 molecule^{-1} s^{-1}, and the uncertainties are 95% confidence limits on the fitting procedure.

The results of the simulation have shown that, under the experimental conditions used, the contribution of reaction 1b to the observed HBr formation was in the range of 50 ±10%. The other part of the observed HBr was due to reaction 33. Thus, the precise knowledge of the rate constant for reaction 33 is very important for the determination of k_{1b}. This rate constant seems to be well established, since the data obtained at room temperature for k_{33} in the three most recent studies are consistent: $k_{33} = (1.98 \pm 0.05) \times 10^{-12}$,[26] $(1.5 \pm 0.2) \times 10^{-12}$,[27] and $(1.7 \pm 0.2) \times 10^{-12}$ cm^3 molecule^{-1} s^{-1}.[24] In the present work, the value measured recently in this laboratory[24] was used in the simulations. The results obtained for k_{1b} were indeed very sensitive to the value of k_{33}: using the values 1.5×10^{-12} and 2.0×10^{-12} cm^3 molecule^{-1} s^{-1} for this rate constant led to changes in the fitted values of k_{1b} within +20% and −30%, respectively.

Another reaction influencing k_{1b} is OH + HBr (eq 34). Its rate constant is well-known: $k_{34} = (1.1 \pm 0.1) \times 10^{-11}$ cm^3 molecule^{-1} s^{-1}, as measured in refs 25 and 28−32 and recommended in refs 1 and 33. Variation of k_{34} within its uncertainty range (±10%) led to changes in k_{1b} within +20% and −6%, respectively. The consumption of HBr by OH has another important consequence in the fitting procedure, since the rate of HBr formation depends on the absolute concentration of HBr

$$d[HBr]/dt = k_{1b}[OH][BrO] + k_{33}[Br][HO_2] - k_{34}[OH][HBr]$$

It means that the kinetics of HBr, from which k_{1b} is derived, depend on the initial concentration of HBr in the reactor (first observation point). In this respect, the signal detected at $m/e = 80$ can be either completely attributed to HBr present in the reactor or partly due to contributions from other species or from the HBr^+ ion formed in the ion source (as a result of homogeneous or heterogeneous chemical processes, for ex-

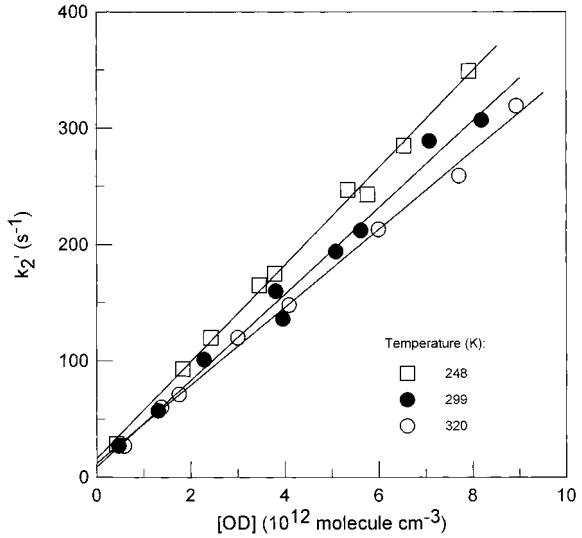

Figure 7. Example of pseudo-first-order plots of BrO consumption in the reaction with excess OD radicals.

ample). In the above calculations, the signal at $m/e = 80$ was considered as corresponding to HBr present in the reactor. Thus, the value obtained for k_{1b} must be considered as the upper limit of the rate constant. Therefore, only the upper limits for k_{1b} and k_{1b}/k_1 are recommended from this study

$$k_{1b} < 1.0 \times 10^{-12}\ \text{cm}^3\,\text{molecule}^{-1}\,\text{s}^{-1}$$

$$k_{1b}/k_1 < 0.03$$

2. Reaction OD + BrO → Products. *a. Kinetic Study.* The rate constant of reaction 2 was measured in a similar way to that of the OH + BrO reaction. The kinetics of BrO consumption were monitored in excess of OD radicals. BrO radicals were formed in the reaction of O atoms with excess Br_2 in the central tube of the movable injector. OD radicals were produced through the reactions of D and F atoms (inlet 3) with NO_2 and D_2O (inlet 4), respectively. When the F + D_2O reaction was used as a source of OD radicals, NO_2 at concentrations of $6-7 \times 10^{13}$ molecules cm^{-3} was also added in the reactor (inlet 4) in order to scavenge oxygen atoms. The initial concentrations of BrO radicals were in the range of $1.5-2.0 \times 10^{11}$molecules cm^{-3}. The concentrations of the precursor species in the reactor were as follows: $[D_2O] = (1-2) \times 10^{14}$ molecules cm^{-3}, and $[Br_2] = 0.5-1.0 \times 10^{12}$ molecules cm^{-3}. Similar to the study of reaction 1, the pseudo-first-order rate constants, $k_2' = -\text{d}(\ln[\text{BrO}])/\text{d}t$, obtained from the BrO consumption kinetics, were corrected for the contribution of the reaction of BrO with NO. Examples of the corrected pseudo first-order plots obtained at different temperatures in the reactor are shown in Figure 7. All the results obtained for k_2 at the different temperatures of the study are reported in Table 5. The temperature dependence of the rate constant of reaction 2 is also shown in Figure 8. These data provide the following Arrhenius expression:

$$k_3 = (1.7 \pm 0.6) \times 10^{-11} \exp\{(230 \pm 100)/T\}\ \text{cm}^3\,\text{molecule}^{-1}\,\text{s}^{-1} \qquad T = (230-320)\ \text{K}$$

where the quoted uncertainties represent 2σ.

b. Mechanistic Study. In the mechanistic study of reaction 2, a procedure similar to that described above for reaction 1 was used. The initial reactants, OD and BrO, were formed in a sequence of reactions conducted in different regions of the main reactor (Figure 2). In region 1, HBr molecules reacted with an excess of atomic fluorine to give Br atoms. D_2/NO_2 mixture was introduced into the reactor through inlet 4. In reaction zone (2), F atoms were completely consumed by an excess of D_2 and D atoms thus formed reacted with NO_2, producing OD radicals. Finally, in region 3, Br atoms reacted with ozone to form BrO radicals. The kinetics of OD, BrO, Br, DO_2, NO, NO_2, DOBr, and DBr were observed experimentally. A reaction mechanism used in the simulation of the experimental profiles is shown in Table 6. The kinetic data for deuterium substituted radicals OD and DO_2 were required for the simulation and are very scarce in the literature. However, in recent studies from this laboratory, the kinetic data for the key reactions involved in the OD + BrO chemical system were measured: reactions of DO_2 with BrO[18] and Br[24] and reactions of OD with DBr,[25] OD,[9] and DO_2 [this work]. For all other reactions of OD and DO_2 (which have negligible impact on the fitting procedure), the known kinetic data for analogous reactions of OH and HO_2 were used. The simulation of the experimental runs shows that this mechanism well represents the chemical processes occurring in the reactor (see Figure 9a). As in the previous case, the two parameters k_{2a} and k_{2b} were determined from the best fit to the experimental kinetics of OD and DBr, respectively. Figure 9b shows the sensitivity of the simulated profiles of DBr to the k_{2b}/k_2 ratio. All the data obtained for k_{2a} and k_{2b} are presented in Table 7, along with the concentrations of OD and BrO used. The initial concentrations of the other species were as follows: $[O_3] = 3.3-9.0 \times 10^{14}$, $[Br_2] = 4.3-11.9 \times 10^{12}$, [NO] = 1.0−

TABLE 5: Reaction OD + BrO → Products (2): Experimental Conditions and Results for the Measurements of the Reaction Rate Constant

T (K)	no/exp.[a]	$[OD]_0$[b]	source of OD	k_1[c]
320	8	0.6−8.9	F + D_2O	3.4 ± 0.8
299	9	0.5−8.2	F + D_2O	3.7 ± 0.9
293	6	0.7−7.3	D + NO_2	3.9 ± 1.0
273	8	0.7−8.8	F + D_2O	3.6 ± 0.9
270	8	0.6−7.9	D + NO_2	4.0 ± 1.0
248	9	0.4−7.9	F + D_2O	4.2 ± 1.1
230	6	0.6−3.4	D + NO_2	4.7 ± 1.2

[a] Number of kinetic runs. [b] Concentrations are in 10^{12} molecules cm^{-3}. [c] Rate constants are in 10^{-11} cm^3 $molecule^{-1}$ s^{-1}, and errors are the conservative 25% uncertainties, including estimated systematic errors.

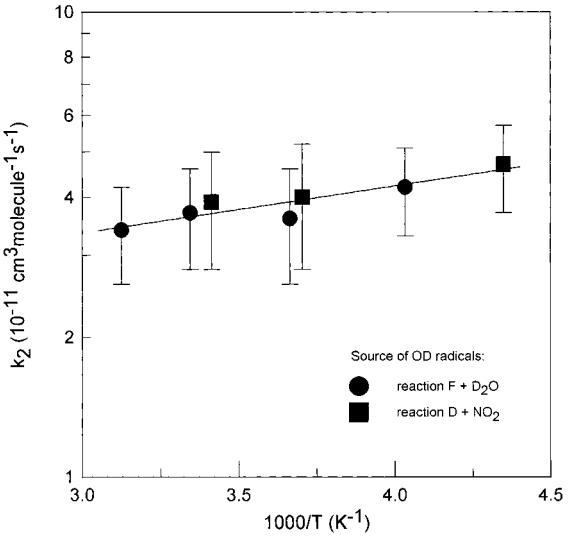

Figure 8. Reaction OD + BrO → products (2): temperature dependence of the reaction rate constant.

TABLE 6: Measurements of the Rate Constant of the Reaction OD + BrO → DBr + O_2 (2b): Mechanism Used in the Computer Simulations

reaction	[a]rate constant	ref
OD + BrO → DBr + O_2	k_{2b}, varied	
OD + BrO → Br + DO_2	k_{2a}, varied	
OD + DO_2 → D_2O + O_2	3.8×10^{-11}	this work
DO_2 + BrO → DOBr + O_2	1.6×10^{-11}	18
DO_2 + Br → DBr + O_2	3.1×10^{-13}	24
DO_2 + NO → OD + NO_2[b]	8.1×10^{-12}	1
DO_2 + O_3 → OD + $2O_2$[b]	2.0×10^{-15}	1
BrO + NO → Br + NO_2	2.1×10^{-11}	1
BrO + BrO → Br + Br + O_2	2.7×10^{-12}	1
BrO + BrO → Br_2 + O_2	0.5×10^{-12}	1
Br + O_3 → BrO + O_2	1.2×10^{-12}	1
OD + O_3 → DO_2 + O_2[b]	6.8×10^{-14}	1
OD + DBr → Br + D_2O	6.5×10^{-12}	25
OD + OD → O + D_2O	4.4×10^{-13}	9
O + OD → D + O_2[b]	3.3×10^{-11}	1
O + DO_2 → OD + O_2[b]	5.9×10^{-11}	1
O + BrO → Br + O_2	4.1×10^{-11}	1
O + NO_2 → NO + O_2	9.7×10^{-12}	1
D + O_3 → OD + O_2[b]	2.9×10^{-11}	1
D + NO_2 → OD + NO	1.2×10^{-10}	9
NO + O_3 → NO_2 + O_2	1.8×10^{-14}	1
BrO + wall → loss	$3\ s^{-1}$	this work
OD + wall → loss	$5\ s^{-1}$	this work
DO_2 + wall → loss	$5\ s^{-1}$	this work

[a] For bimolecular reactions, the units are cm^3 $molecule^{-1}$ s^{-1}; all rate constants are at $T = 298$ K. [b] For these reactions, the rate constants of the analogous reactions of OH and HO_2 were used.

7.1×10^{13}, and $[NO_2] = 0.4-1.5 \times 10^{14}$ molecules cm^{-3}. The mean value of $k_{2a} = (3.8 \pm 0.8) \times 10^{-11}$ cm^3 $molecule^{-1}$ s^{-1} obtained from six experiments is in excellent agreement with that obtained above more directly: $k_2 = (3.7 \pm 0.9) \times 10^{-11}$ cm^3 $molecule^{-1}$ s^{-1}.

The analysis of the kinetic runs of DBr shows that 60−80% of DBr formed was due to reaction 2b and that the remaining part resulted from the DO_2 + Br reaction

$$DO_2 + Br \rightarrow DBr + O_2 \quad (35)$$

$$k_{35} = 4.9 \times 10^{-12} \exp(-310/T)\ cm^3\ molecule^{-1}\ s^{-1}\ [24]$$

with $k_{35} = (3.1 \pm 0.6) \times 10^{-13}$ at $T = 298$ K. Another reaction which could influence the observed kinetics of DBr was reaction 36

$$OD + DBr \rightarrow Br + D_2O \quad (36)$$

$$k_{36} = 5.3 \times 10^{-12} \exp(225/T)\ cm^3\ molecule^{-1}\ s^{-1}\ [25]$$

with $k_{36} = (6.5 \pm 1.8) \times 10^{-12}$ cm^3 $molecule^{-1}$ s^{-1}. The sensitivity analysis has shown that the variation of k_{35} in the limits of the quoted uncertainty led to changes in k_{2b} within ±15%. Variation of k_{36} by a factor of 2 led to the modification of the fitted value of k_{2b} from −10% to +30%. It is important to note that the results obtained for k_{2b} are much less sensitive to the rate constant of the reaction OD + DBr (i.e., less sensitive to the absolute level of DBr concentrations) than those for k_{1b} to the rate constant of the reaction OH + HBr in the study of OH + BrO reaction. This is due to (i) much lower concentrations of DBr than HBr being detected (lower DBr background) and (ii) the rate constant of the OD + DBr reaction being lower by a factor 1.7 than that of the analogous OH + HBr reaction. Finally, taking into account the results of the sensitivity analysis as well as the accuracy of the measurements of the low

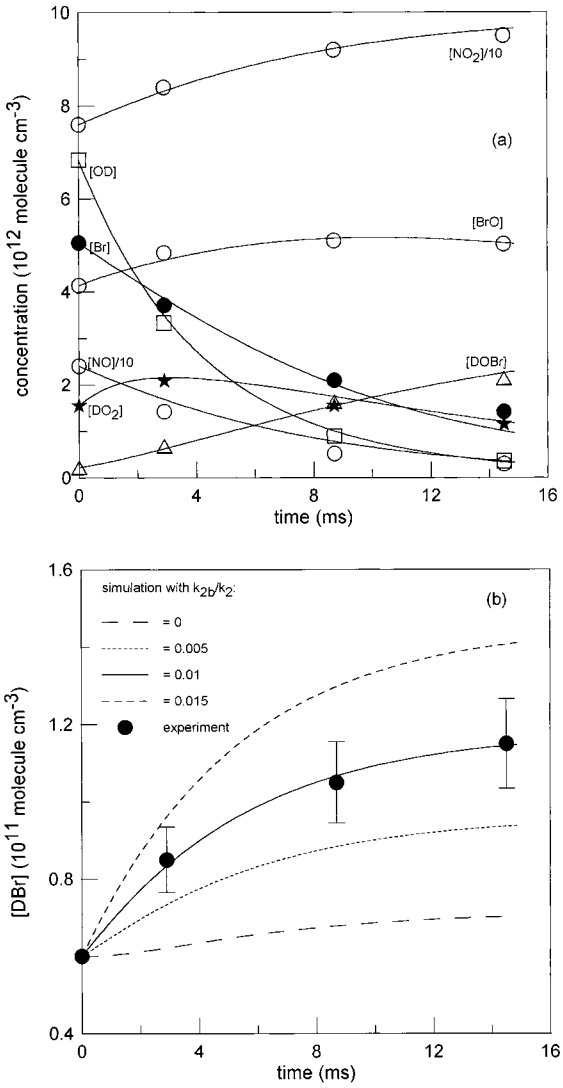

Figure 9. Example of experimental (points) and simulated (lines) kinetics for the species detected in the chemical system used for the study of the reaction OD + BrO → DBr + O_2 (2b): $t = 0$ corresponds to the first observation point at the top of the reaction zone (see text for Figure 9,b).

TABLE 7. Measurements of the Rate Constant for the Reaction OD + BrO → DBr + O_2 (2b): Experimental Conditions and Results

no	[OD][a]	[BrO][a]	$k_{2a}/10^{-11}$ [b]	$k_{2b}/10^{-13}$ [b]
1	3.6	10.6	3.1 ± 0.7	3.1 ± 0.8
2	6.8	4.1	3.8 ± 0.6	3.5 ± 0.3
3	6.9	3.1	3.9 ± 0.2	3.8 ± 0.2
4	8.3	4.4	3.9 ± 0.7	3.0 ± 0.3
5	8.7	2.3	3.6 ± 0.2	4.1 ± 0.2
6	9.5	3.5	4.7 ± 0.6	4.6 ± 0.3

[a] Concentrations are in 10^{12} molecules cm^{-3}, and the concentrations represent those measured at the top of the reaction zone (first observation point). [b] Rate constants are in cm^3 $molecule^{-1}$ s^{-1}, and the uncertainties are 95% confidence limits on the fitting procedure.

concentrations of DBr, we recommend the following value of k_{2b} at $T = 298$ K from this study (rather than an upper limit)

$$k_{2b} = (3.7 \pm 1.8) \times 10^{-13}\ cm^3\ molecule^{-1}\ s^{-1}$$

(where uncertainty represent 95% confidence limits and includes estimated systematic errors). This corresponds to the following

value of the branching ratio for DBr-forming channel of reaction 2

$$k_{2b}/k_2 = (1.0 \pm 0.5) \times 10^{-2}$$

3. Reaction OD + DO_2 → D_2O + O_2. This reaction has been investigated as a part of the OD + BrO reaction study. Kinetic information on reaction 3 was needed for the simulation of the experimental data in the mechanistic study of reaction 2, as this reaction has a direct impact on the kinetics of the two key species involved in DBr formation and consumption (OD and DO_2).

Reaction of F atoms with excess D_2O_2/D_2O mixture (30% D_2O_2 in D_2O) was used to form DO_2 and OD radicals

$$F + D_2O_2 \rightarrow DO_2 + DF \quad (22)$$

$$F + D_2O \rightarrow OD + DF \quad (8)$$

Other active species which could be produced in these sources of the radicals were O and D atoms, resulting from the secondary reactions

$$F + OD \rightarrow O + DF \quad (37)$$

$$OD + OD \rightarrow O + D_2O \quad (11)$$

$$O + OD \rightarrow D + O_2 \quad (38)$$

To avoid any complication which could arise from the secondary chemistry initiated by O and D atoms, we added NO_2 into the reactor ($[NO_2] = 0.5-1.0 \times 10^{14}$ molecules cm^{-3}), which led to scavenging of the O and D atoms through reactions 27 and 7, respectively. Thus, the reactive species entering the reactor from the source of the radicals were OD, DO_2, NO, NO_2, and D_2O_2. All these species were detected and quantified by mass spectrometry. Under the experimental conditions used, an excess of OD over DO_2 was always observed, and the rate constant of reaction 3 was determined from the kinetics of DO_2 consumption. The observed decays of DO_2 were due to the following processes: reaction 3 with OD, reaction 23 with NO, and heterogeneous loss of DO_2 radicals (k_w). Therefore, the pseudo-first-order rate constant determined from the exponential fit to the experimental kinetics of DO_2 consumption was $k_3'_{measured} = k_3[OD] + k_{23}[NO] + k_w$. The values of $k_3'_{measured}$ were corrected for the axial and radial diffusion of DO_2. The diffusion coefficient of DO_2 in He was calculated from that of O_2 in He.[20] The corrections were less than 7%. The contribution of reaction 23, $k_{23}[NO]$, could be easily extracted (the concentration of NO in the reactor was measured, and for k_{23}, the value of the rate constant for the analogous HO_2 + NO reaction was used: 8.1×10^{-13} cm^3 $molecule^{-1}$ s^{-1} [1]). The maximum correction on $k_3'_{measured}$ due to this contribution was 12%. The results thus obtained for $k_3' = k_3[OD] + k_w$ are presented in Figure 10. The variation of the initial concentration of OD radicals was achieved by variation of the concentrations of D_2O_2/D_2O and F atoms. A consumption (up to 50% in a few kinetic runs) of the excess reactant, OD radicals, was observed. Concentrations of OD shown in Figure 10 are the mean values of [OD] along the reaction zone. Linear fit to the experimental data presented in Figure 10 provides the following value of the rate constant for OD + DO_2 reaction at $T = 298$ K:

$$k_3 = (3.8 \pm 0.9) \times 10^{-11} \text{ cm}^3 \text{ molecule}^{-1} \text{ s}^{-1}$$

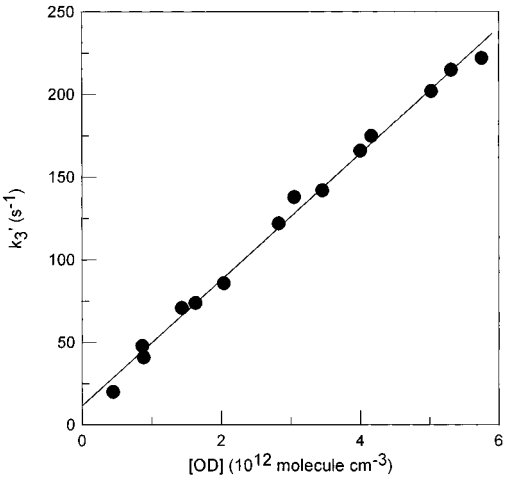

Figure 10. Reaction OD + DO_2 → products (3): pseudo-first-order plot of DO_2 consumption in reaction with excess OD radicals.

(where uncertainty represent 95% confidence limits and includes estimated systematic errors).

The presence of D_2O_2 in the reactor could lead to the regeneration of DO_2 radicals in reaction 39

$$OD + D_2O_2 \rightarrow DO_2 + D_2O \quad (39)$$

$k_{39} = (6.0 \pm 1.0) \times 10^{-13}$ cm^3 $molecule^{-1}$ s^{-1} at $T =$ 298 K [34].

However, under the experimental conditions used ($[D_2O_2] \approx 1.0 \times 10^{12}$ and $[DO_2]_0 = (0.5-1.0) \times 10^{12}$ molecules cm^{-3}), the ratio $k_{39}[D_2O_2]/k_3[DO_2]$ was always $\ll 1$; i.e., the rate of DO_2 consumption by OD was always much higher than the rate of its formation in reaction of OD with D_2O_2. Thus, the possible impact of this DO_2 regeneration on the results of the measurements of k_3 can be neglected considering the uncertainty given for k_3.

The value of k_3 can be compared with that for the analogous reaction between OH and HO_2 radicals: $k_{31} = (1.1 \pm 0.3) \times 10^{-10}$ cm^3 $molecule^{-1}$ s^{-1} at $T = 298$ K.[1] The isotopic effect is $k_{31}/k_3 \approx 2.9$. It is interesting to compare the observed kinetic isotope effect with that known for the reactions OH + OH, OH + H_2O_2 and HO_2 + HO_2

$$OH + OH \rightarrow H_2O + O \quad (10)$$

$$OD + OD \rightarrow D_2O + O \quad (11)$$

$$OH + H_2O_2 \rightarrow HO_2 + H_2O \quad (21)$$

$$OD + D_2O_2 \rightarrow \text{products} \quad (39)$$

$$HO_2 + HO_2 \rightarrow H_2O_2 + O_2 \quad (40)$$

$$DO_2 + DO_2 \rightarrow D_2O_2 + O_2 \quad (41)$$

The isotopic effects determined for these reactions—$k_{10}/k_{11} = 3.2$ [9], $k_{21}/k_{39} = 3.3$ [34], and $k_{40}/k_{41} = 2.8$ [35] and 3.3 [36]—are similar to that observed in the present study: $k_{31}/k_3 \approx 2.9$.

Discussion

Reaction 1 between OH and BrO has been investigated in only one previous study by Bogan et al.[8] These experiments were also carried out in a discharge flow system with beam-

sampling mass spectrometry. The rate constant for reaction 1 was obtained from the numerical simulation of the observed temporal profiles of BrO. The value found for k_1 was $(7.5 \pm 4.2) \times 10^{-11}$ cm^3 molecule^{-1} s^{-1} at $T = 300$ K and 1 Torr total pressure. This value is higher than that measured in the present study by a factor of 2, although the two values overlap considering the relatively high uncertainty range given in ref 8. The reaction between OD and BrO radicals has been investigated for the first time in the present study. Similar data were obtained for the rate constants of reactions 1 and 3. A negligible isotopic effect could be expected for the studied reactions, since the OH(OD) bond is not involved in the chemical transformation.

To our knowledge, no experimental mechanistic study of the OH + BrO reaction has been carried out previously. However, this reaction has been the subject of a recent theoretical study of Sumathi and Peyerimhoff.[37] HOOBr was found to be the most stable isomer (33.8 kcal mol^{-1} below the reactants) of the adducts which can be formed from the OH and BrO association. It was also shown that the barrier for the HBr formation from this adduct is very high (~39 kcal mol^{-1} above the HOOBr intermediate). As a result, the HBr formation in the reaction OH + BrO was predicted to be of importance only at temperatures above 2000 K. This is in disagreement with the present study where HBr (at least DBr in reaction 2) formation in reaction 1 was unambiguously observed at $T =$ 298 K.

The atmospheric implications of the present kinetic data can be briefly discussed. The potential role of the reaction OH + BrO has already been investigated in two modeling studies,[5,6] where it was shown that even with a very low yield of HBr (1−2%[5] and 2−3%[6]), reaction 1b should be the dominant source of HBr at altitudes between 20 and 35 km. Moreover, this will reconcile model calculations with the results of stratospheric HBr observations.[7,38,39] In both studies (refs 5 and 6), the rate constant $k_1 = 7.5 \times 10^{-11}$ cm^3 molecule^{-1} s^{-1} measured by Bogan et al.[8] was used in the calculations. That means that 1% yield of HBr corresponded to the partial rate constant $k_{1b} = 7.5 \times 10^{-13}$ cm^3 molecule^{-1} s^{-1}. This value can be compared with the experimental value obtained in the present study: $k_{1b} < 1.0 \times 10^{-12}$ cm^3 molecule^{-1} s^{-1}. As one can see, the experimental upper limit for of k_{1b} does not contradict with that proposed by Chipperfield et al.[5] to account for the difference between the measured and calculated HBr profiles. A comparison can be also made with the experimental data obtained for the OD + BrO reaction. However, in this case, two assumptions should be made: the branching ratio for HBr formation in OH + BrO reaction is independent of temperature and similar to that for the DBr-forming channel of the reaction OD + BrO. These assumptions seem to be reasonable, considering that they hold for the analogous reactions of ClO radicals with OH and OD.[40,41] Thus, the 1% yield of DBr measured in the present work and the value of the total rate constant $k_1 \approx 5 \times 10^{-11}$ cm^3 molecule^{-1} s^{-1} (at $T = 220-230$ K) gives $k_{1b} \approx 5 \times 10^{-13}$ cm^3 molecule^{-1} s^{-1} at altitudes of 20−35 km. This value is lower than that used in the model calculations ($k_{1b} = 7.5 \times 10^{-13}$ cm^3 molecule^{-1} s^{-1})[5] by a factor 1.5, although both values overlap if the uncertainty of 50% on the branching ratio k_{2b}/k_2 is considered. In conclusion, the present work gives an experimental evidence for the occurrence of HBr formation in the OH + BrO reaction. However, the impact of this reaction on the total HBr budget in the stratosphere seems to be less important than currently predicted by the models due to (i) a lower value for the total rate constant than that used in the calculations and (ii) the value of the branching ratio for HBr formation (1%), which is the low limit of the range proposed by the models (1−3%). Finally, it is difficult to make definitive conclusion from this work if the additional HBr source from the OH + BrO reaction, although significant, will be sufficient to explain the difference between current modeled and observed stratospheric HBr concentrations, since the uncertainties on the kinetic data obtained here and the existing numerical simulations overlap.

Acknowledgment. This study is a part of the project funded by the European Commission within the ≪Environment and Climate≫ Program (Contract ENV - CT97 - 0576, "COBRA").

References and Notes

(1) De More, W. B.; Sander, S. P.; Golden, D. M.; Hampson, R. F.; Kurylo, M. J.; Howard, C. J.; Ravishankara, A. R.; Kolb, C. E.; Molina, M. J. *Chemical Kinetics and Photochemical Data for Use in Stratospheric Modeling*; NASA, JPL; California Institute of Technology: Pasadena, CA, 1997.

(2) Hills, A. J.; Howard, C. J. *J. Chem. Phys.* **1984**, *81*, 4458.

(3) Bedjanian, Y.; Riffault, V.; Le Bras, G. *Int. J. Chem. Kinet.*, submitted for publication.

(4) Bedjanian, Y.; Le Bras, G.; Poulet, G. *Chem. Phys. Lett.* **1997**, *266*, 233.

(5) Chipperfield, M. P.; Shallcross, D. E.; Lary, D. J. *Geophys. Res. Lett.* **1997**, *24*, 3025.

(6) Chartland, D. J.; McConnell, J. C. *Geophys. Res. Lett.* **1998**, *25*, 55.

(7) Nolt, I. G.; Ade, P. A. R.; Alboni, F.; Carli, B.; Carlotti, M.; Cortesi, U.; Epifani, M.; Griffin, M. J.; Hamilton, P. A.; Lee, C.; Lepri, G.; Mencaraglia, F.; Murray, A. G.; Park, J. H.; Park, K.; Raspollini, P.; Ridolfi, M.; Vanek, M. D. *Geophys. Res. Lett*. **1997**, *24*, 281.

(8) Bogan, D. J.; Thorn, R. P.; Nesbitt, F. L.; Stief, L. J. *J. Phys. Chem.* **1996**, *100*, 14838.

(9) Bedjanian, Y.; Le Bras, G.; Poulet, G. *J. Phys. Chem. A* **1999**, *103*, 7017.

(10) Stevens, P. S.; Brune, W. H.; Anderson, J. G. *J. Phys. Chem.* **1989**, *93*, 4068.

(11) Persky, A.; Kornweitz, H. *Int. J. Chem. Kinet.* **1977**, *29*, 68.

(12) Bedjanian, Y.; Le Bras, G.; Poulet, G. *Int. J. Chem. Kinet.* **1999**, *31*, 698.

(13) Nicovich, J. M.; Wine, P. H. *Int. J. Chem. Kinet.* **1990**, *22*, 379.

(14) Edrei, R.; Persky, A. *Chem. Phys. Lett.* **1989**, *157*, 265.

(15) Walther, C. D.; Wagner, H. G. *Ber. Bunsen-Ges. Phys. Chem.* **1983**, *87*, 403.

(16) Glaschick-Schimpf, I.; Leiss, A.; Monkhouse, P. B.; Schurath, U.; Becker, K. H.; Fink, E. H. *Chem. Phys. Lett.* **1979**, *67*, 318.

(17) Wada, Y.; Takayanagi, T.; Umemoto, H.; Tsunashima, S.; Sato, S. *J. Chem. Phys.* **1991**, *94*, 4896.

(18) Bedjanian, Y.; Riffault, V.; Le Bras, G.; Poulet, G. *J. Phys. Chem. A* **2001**, *105*, 3167.

(19) Kaufman, F. *J. Phys. Chem.* **1984**, *88*, 4909.

(20) Morrero, T. R.; Mason, E. A. *J. Phys. Chem. Ref. Data* **1972**, *1*, 3.

(21) Mallard, W. G.; Westley, F.; Herron, J. T.; Frizzell, D.; Hampson, R. F. *NIST Chemical Kinetics Data Base*, ver. 17-2Q98; NIST Standard Reference Data: Gaithersburg, MD, 1998.

(22) Bossard, A. R.; Singleton, D. L.; Paraskevopoulos, G. *Int. J. Chem. Kinet.* **1988**, *20*, 609.

(23) Gilles, M. K.; Burkholder, J. B.; Ravishankara, A. R. *Int. J. Chem. Kinet.* **1999**, *31*, 417.

(24) Bedjanian, Y.; Riffault, V.; Le Bras, G.; Poulet, G. *J. Phys. Chem. A* **2001**, *105*, 573.

(25) Bedjanian, Y.; Riffault, V.; Le Bras, G.; Poulet, G. *J. Photochem. Photobiol., A: Chemistry* **1999**, *128*, 15.

(26) Toohey, D. W.; Brune, W. H.; Anderson, J. G. *J. Phys. Chem.* **1987**, *91*, 1215.

(27) Laverdet, G.; Le Bras, G.; Mellouki, A.; Poulet, G. *Chem. Phys. Lett.* **1990**, *172*, 430.

(28) Ravishankara, A. R.; Wine, P. H.; Langford, A. O. *Chem. Phys. Lett.* **1979**, *63*, 479.

(29) Jourdain, J. L.; Le Bras, G.; Combourieu, J. *Chem. Phys. Lett.* **1981**, *78*, 483.

(30) Cannon, B. D.; Robertshaw, J. S.; Smith, I. W. M.; Williams, M. D. *Chem. Phys. Lett.* **1984**, *105*, 380.

(31) Ravishankara, A. R.; Wine, P. H.; Wells, J. R. *J. Chem. Phys.* **1985**, *83*, 447.

(32) Sims, I. R.; Smith, I. W. M.; Clary, D. C.; Bocherel, P.; Rowe, B. R. *J. Chem. Phys.* **1994**, *101*, 1748.
(33) Atkinson, R.; Baulch, D. L.; Cox, R. A.; Hampson, R. F.; Kerr, J. A.; Rossy, M. J.; Troe, J. *J. Phys. Chem. Ref. Data* **1997**, *26*, 521.
(34) Vaghjiani, G. L.; Ravishankara, A. R.; Cohen, N. *J. Phys. Chem.* **1989**, *93*, 7833.
(35) Hamilton, E. J.; Lii, R.-R. *Int. J. Chem. Kinet.* **1977**, *9*, 875.
(36) Sander, S. P.; Peterson, M.; Watson, R. T. *J. Phys. Chem.* **1982**, *86*, 1236.
(37) Sumathi, R.; Peyerimhoff, S. D. *Phys. Chem. Chem. Phys.* **1999**, *1*, 3973.
(38) Carlotti, M.; et al. *Geophys. Res. Lett.* **1995**, *22*, 3207.
(39) Johnson, D. G.; Traub, W. A.; Chance, K. V.; Jucks, K. W. *Geophys. Res. Lett.* **1995**, *22*, 1373.
(40) Lipson, J. B.; Elrod, M. J.; Beiderhase, T. W.; Molina, L. T.; Molina, M. J. *J. Chem. Soc., Faraday Trans.* **1997**, *93*, 2665.
(41) Lipson, J. B.; Beiderhase, T. W.; Molina, L. T.; Molina, M. J.; Olzmann, M. *J. Phys. Chem. A* **1999** *103*, 6540.